J. Fluid Mech. (1983), *vol.* 133, *pp.* 65–81
Printed in Great Britain

Flow past a liquid drop with a large non-uniform radial velocity

By S. S. SADHAL
Department of Mechanical Engineering, University of Southern California, Los Angeles, CA 90089-1453

AND P. S. AYYASWAMY
Department of Mechanical Engineering and Applied Mechanics, University of Pennsylvania, Philadelphia, PA 19104

(Received 1 October 1982 and in revised form 1 February 1983)

In this analysis, the translation of a liquid drop experiencing a strong non-uniform radial velocity has been investigated. The situation arises when a moving liquid drop experiences condensation, evaporation or material decomposition at the surface. By simultaneously treating the flow fields inside and outside the drop, we have obtained physical results relevant to the problem. The magnitude of the radial velocity is allowed to be very large, but the drop motion is restricted to slow translation. The solution to the problem has been developed by considering a uniform radial flow with the translatory motion introduced as a perturbation. The role played by the inertial terms due to the strong radial field has been clearly delineated. The study has revealed several interesting features. An inward normal velocity on a slowly moving drop increases the drag. An increasing outward normal velocity decreases the drag up to a minimum beyond which it increases. The total drag force not only consists of contributions from the viscous and the form drags but also from the momentum transport at the interface. Since the liquid drop admits a non-zero tangential velocity, the tangential momentum convected by the radial velocity forms a part of this drag force. The circulation inside the drop decreases (increases) with an outward (inward) normal velocity. A sufficiently large non-uniform outward velocity causes the circulation to reverse.

In the limit of the internal viscosity becoming infinite, our analysis collapses to the simple case of a translating rigid sphere experiencing a large non-uniform radial velocity. By letting the radial velocity become vanishingly small the Stokes-flow solution is recovered.

An important contribution of the present study is the identification of a new singularity in the flow description. It accounts for both the inertial and the viscous forces and displays Stokeslet-like characteristics at infinity.

1. Introduction

In this paper we examine the flow fields associated with the translation of a liquid drop experiencing internal circulation in the presence of a large non-uniform radial velocity. This situation arises, for example, when there is a rapid change of phase or material decomposition at the interface. In the area of liquid-spray cooling, large normal velocities are encountered owing to condensation on moving drops. For evaporating liquid aerosols, large radially outward velocities are observed. The oxidation near the interface of a burning spray fuel drop often results in the net production of a gas, leading to a large radial field (see Law 1982). These areas of application would benefit from the understanding of the detailed fluid mechanics governing the external forced flow and its coupling with the internal circulation. In particular, knowledge of the drag force and the strength of the internal vortex is of fundamental interest for the further development of these areas.

The analysis here calls for the simultaneous solution of the flow fields in the dispersed and the continuous phases. The coupling of the two phases at the interface requires the inclusion of the viscous forces. In addition, the presence of the large normal velocity at the interface leads to significant inertial forces. The earliest examinations of the coupled problem with an impenetrable but mobile interface include the classical papers by Rybczynski (1911) and Hadamard (1911). Further studies on drop deformation were carried out by Saito (1913) and by Taylor & Acrivos (1964). The case of a non-zero normal velocity has been treated by Fendell, Sprankle & Dodson (1966), Gal-Or & Yaron (1973) and Schneider (1981). All of these solutions are valid strictly for the Stokes-flow regime and hence cannot accommodate a large radial field. Excellent reviews in the area of moving drops have been given by Clift, Grace & Weber (1978) and by Harper (1972). The literature on the problem related to the motion of a rigid sphere is quite extensive and will not be reviewed here. However, it is noteworthy that the problem of a translating rigid sphere experiencing a large non-uniform radial flow is a special case of our analysis when the internal viscosity becomes infinite.

Although a large uniform radial flow is an exact solution to the full Navier–Stokes equations, it cannot be superimposed on the Hadamard–Rybczynski flow even for a slowly translating drop. This is because of the importance of the nonlinear inertial terms whenever the radial field is large. In this paper the effects of a strong normal velocity are examined by retaining both the viscous and the inertial terms. We do this by considering a drop with a purely radial field and by subsequently introducing the translation as a small perturbation. A regular perturbation scheme is used to calculate the first-order correction. This correction is found to be uniformly valid.

Several important results are obtained from this solution. In particular, analytical expressions are given for the drag force and the strength of the internal vortex. The detailed analysis reveals a very interesting behaviour of these quantities. The drag force decreases with increasing outward non-uniform velocity up to a minimum, beyond which it increases. An increasing inward normal velocity consistently increases the drag. Also, with a large enough outward velocity, the internal circulation within the drop reverses its direction of motion. A detailed discussion on the various mechanisms that participate in the characterization of such behaviour is given later. While the present contribution deals with the fundamental aspects of the fluid dynamics, specific applications to heat and mass transfer associated with a translating liquid drop are given in forthcoming publications (see e.g. Chung, Ayyaswamy & Sadhal 1983*a*, *b*).

2. Statement of problem

We consider a liquid drop of radius R with a uniform normal velocity A_0 at the outer surface. The drop translates at a velocity U_∞ in a gaseous medium. In addition to the uniform velocity A_0, the radial field is enhanced by an amount $a_1(\theta)$ due to translational effects (see figure 1). The shape of the drop is taken to remain spherical. The drop deformation for many situations of interest can be shown to be insignificant

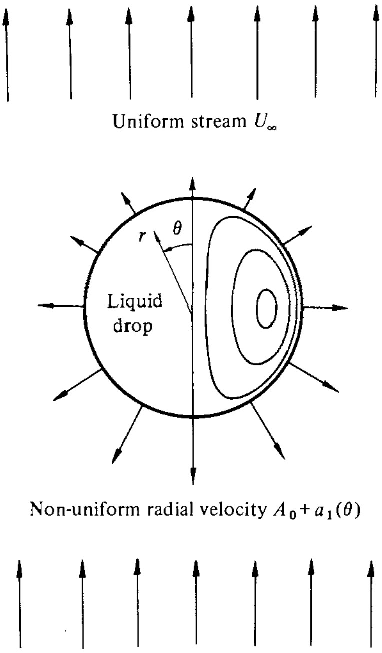

FIGURE 1. A schematic of the flow problem under investigation.

(Clift *et al.* 1978). A spherical coordinate system, with the origin at the centre of the drop, is employed to formulate the governing equations. The inside of the drop ($0 \leqslant r < R$) is distinguished from the outside ($R < r < \infty$) by a 'hat' ($\hat{}$). The flow is axially symmetric with velocity $\boldsymbol{u}(r, \theta)$ having two components (u_r, u_θ).

The velocity fields in both the dispersed and the continuous phases are taken to be quasisteady. The quasisteady aspect can be easily justified in view of the large ratio of the liquid to the gas phase densities. The implication of the large density ratio is that the rate of change of the liquid volume due to the interfacial transport is small, even though the radial velocity A_0 may be large. The rate of change of the drop radius is of order

$$\dot{R} = A_0 \frac{\rho}{\hat{\rho}}, \tag{1}$$

where ρ and $\hat{\rho}$ are the densities of the continuous and the dispersed phases respectively. The timescale governing substantial change in the drop size is therefore

$$t_{\dot{R}} = \frac{R}{\dot{R}} = \frac{\hat{\rho}}{\rho} \frac{R}{A_0}. \tag{2}$$

On the other hand, a typical diffusion time is

$$t_\nu = \frac{R^2}{\nu}, \tag{3}$$

where ν is the kinematic viscosity of the continuous phase.

In order that we may neglect the transient effects due to size changes, $t_\nu \ll t_{\dot{R}}$, or

$$A_{00} = \frac{A_0 R}{\nu} \ll \frac{\hat{\rho}}{\rho}. \tag{4}$$

With the high density ratio $\hat{\rho}/\rho \approx 10^3$ for most liquid–gas systems, the radial Reynolds number A_{00} may be as large as 10. Under these conditions, the quasisteady approximation for the velocity field is valid. Also because of the large density ratio, the normal velocity on the liquid side of the surface is negligibly small. It is therefore assumed that the radial velocity on the inner side of the interface vanishes.

The governing equations for this system are

continuity:

$$\nabla \cdot \boldsymbol{u} = 0, \tag{5}$$

$$\nabla \cdot \hat{\boldsymbol{u}} = 0; \tag{6}$$

momentum:

$$\rho \boldsymbol{u} \cdot \nabla \boldsymbol{u} + \nabla p = \mu \nabla^2 \boldsymbol{u}, \tag{7}$$

$$\hat{\rho} \hat{\boldsymbol{u}} \cdot \nabla \hat{\boldsymbol{u}} + \nabla \hat{p} = \hat{\mu} \nabla^2 \hat{\boldsymbol{u}}. \tag{8}$$

The boundary conditions are

(i) uniform stream at infinity:

$$u_r = U_\infty \cos\theta, \quad u_\theta = -U_\infty \sin\theta; \tag{9a}$$

(ii) normal velocity:

$$u_r|_{r=R} = A_0 + a_1(\theta), \quad \hat{u}_r|_{r=R} = 0; \tag{9b}$$

(iii) continuity of tangential velocity:

$$u_\theta|_{r=R} = \hat{u}_\theta|_{r=R}; \tag{9c}$$

(iv) continuity of shear stress:

$$\mu\left[r\frac{\partial}{\partial r}\left(\frac{u_\theta}{r}\right) + \frac{1}{r}\frac{\partial u_r}{\partial \theta}\right]_{r=R} = \hat{\mu}\left[r\frac{\partial}{\partial r}\left(\frac{\hat{u}_\theta}{r}\right) + \frac{1}{r}\frac{\partial \hat{u}_r}{\partial \theta}\right]_{r=R}; \tag{9d}$$

(v) finite velocity at the origin:

$$\hat{\boldsymbol{u}}|_{r\to 0} < \infty. \tag{9e}$$

The translation-induced normal velocity $a_1(\theta)$ in (9*b*) is treated as an arbitrary parameter which may be determined by the prevailing thermodynamics of system. However, in many situations involving interfacial transport, it has the same characteristics as the translational field (see Chung *et al.* 1983*a*). Hence we shall examine a velocity variation of the type

$$a_1(\theta) = a_{01} + a_{11}\cos\theta. \tag{10}$$

The enhancement due to translation is more pronounced at the front stagnation point ($\theta = \pi$, see figure 1), and the maximum value of $|a_1(\theta)|$ occurs there. The sign of a_{11} is thus opposite to that of A_0 and a_{01}.

3. Solution by perturbation

Let the leading-order velocity field be a purely radial flow with a velocity A_0 at the surface. In the absence of translation the velocity $\boldsymbol{u}_0$ is

$$\boldsymbol{u}_0 = A_0 \frac{R^2}{r^2} \hat{\boldsymbol{r}}, \tag{11}$$

where $\hat{\boldsymbol{r}}$ is a unit vector in the radial direction. To account for translation, corrections $\boldsymbol{u}'$ and $\hat{\boldsymbol{u}}'$ are implemented, viz

$$\boldsymbol{u} = \boldsymbol{u}_0 + \boldsymbol{u}', \tag{12}$$

$$\hat{\boldsymbol{u}} = \hat{\boldsymbol{u}}_0 + \hat{\boldsymbol{u}}', \tag{13}$$

where $\hat{\boldsymbol{u}}_0$ is equal to zero. The corresponding pressures may be written as

$$p = p_0 + p', \tag{14}$$

$$\hat{p} = \hat{p}_0 + \hat{p}', \tag{15}$$

where $\hat{p}_0$ is a constant.

In order to non-dimensionalize the governing equations it is appropriate to scale $\boldsymbol{u}_0$ with A_0, and $\boldsymbol{u}'$ and $\hat{\boldsymbol{u}}'$ with U_∞. Thus $\boldsymbol{u}_0^* = \boldsymbol{u}_0/A_0$, $\boldsymbol{u}'^* = \boldsymbol{u}'/U_\infty$, $\hat{\boldsymbol{u}}'^* = \hat{\boldsymbol{u}}'/U_\infty$, $A_{01} + A_{11}\cos\theta = (a_{01} + a_{11}\cos\theta)/U_\infty$, $r^* = r/R$, $\epsilon = U_\infty R/\nu$, $A_{00} = A_0 R/\nu$, $\phi_\mu = \mu/\hat{\mu}$, $\phi_\nu = \nu/\hat{\nu} = (\mu/\rho)/(\hat{\mu}/\hat{\rho})$, $p_0^* = p_0/(A_0\mu/R)$, $p'^* = p'/(U_\infty\mu/R)$, $\hat{p}'^* = \hat{p}/(U_\infty\hat{\mu}/R)$, and $\boldsymbol{\nabla}^* = R\boldsymbol{\nabla}$. By defining a non-dimensional velocity in the gas phase as $\boldsymbol{u}^* = \boldsymbol{u}R/\nu$, we may write

$$\boldsymbol{u}^* = A_{00}\boldsymbol{u}_0^* + \epsilon\boldsymbol{u}'^*. \tag{16}$$

Similarly, with $\hat{\boldsymbol{u}}^* = \hat{\boldsymbol{u}}R/\nu$ it is easy to see that

$$\hat{\boldsymbol{u}}^* = \widehat{Re}\,\hat{\boldsymbol{u}}'^* \tag{17}$$

where $\widehat{Re} = U_\infty R/\hat{\nu}$ is the Reynolds number for the liquid phase. The pressure is scaled in a similar fashion. In the gas (vapour) phase, with $p^* = pR^2/\mu\nu$ we obtain

$$p^* = A_{00}p_0^* + \epsilon p'^*. \tag{18}$$

The pressure in the liquid phase may be scaled with $\hat{\mu}\hat{\nu}/R^2$ to yield

$$\hat{p}^* = \hat{A}_{00}\hat{p}_0^* + \widehat{Re}\,\hat{p}'^* \tag{19}$$

where $\hat{A}_{00} = A_0 R/\hat{\nu}$.

The non-dimensional governing equations (with the asterisks omitted) are continuity:

$$\boldsymbol{\nabla}\cdot(A_{00}\boldsymbol{u}_0 + \epsilon\boldsymbol{u}') = 0, \tag{20}$$

$$\boldsymbol{\nabla}\cdot(\epsilon\hat{\boldsymbol{u}}') = 0; \tag{21}$$

momentum:

$$A_{00}^2\boldsymbol{u}_0\cdot\boldsymbol{\nabla}\boldsymbol{u}_0 + A_{00}\epsilon(\boldsymbol{u}_0\cdot\boldsymbol{\nabla}\boldsymbol{u}' + \boldsymbol{u}'\cdot\boldsymbol{\nabla}\boldsymbol{u}_0) + \epsilon^2\boldsymbol{u}'\cdot\boldsymbol{\nabla}\boldsymbol{u}' + A_{00}\boldsymbol{\nabla}p + \epsilon\boldsymbol{\nabla}p' = A_{00}\nabla^2\boldsymbol{u}_0 + \epsilon\nabla^2\boldsymbol{u}', \tag{22}$$

$$\widehat{Re}\,\hat{\boldsymbol{u}}'\cdot\boldsymbol{\nabla}\hat{\boldsymbol{u}}' + \boldsymbol{\nabla}\hat{p}' = \nabla^2\hat{\boldsymbol{u}}'; \tag{23}$$

boundary conditions:

$$\left.\begin{aligned} [u_{0r} + \epsilon u_r']_{r\to\infty} &= \epsilon\cos\theta, \\ [u_{0\theta} + \epsilon u_\theta']_{r\to\infty} &= -\epsilon\sin\theta, \end{aligned}\right\} \tag{24a}$$

$$\left.\begin{aligned} [A_{00}u_{0r} + \epsilon u_r']_{r=1} &= A_{00} + \epsilon[A_{01} + A_{11}\cos\theta], \\ \hat{u}_r'|_{r=1} &= 0, \end{aligned}\right\} \tag{24b}$$

$$[A_{00}u_{0\theta} + \epsilon u_\theta']_{r=1} = \epsilon\hat{u}_\theta', \tag{24c}$$

$$\phi_\mu\left[r\frac{\partial}{\partial r}\left(\frac{A_{00}u_{0\theta} + \epsilon u_\theta'}{r}\right) + \frac{1}{r}\frac{\partial}{\partial\theta}(A_{00}u_{0r} + \epsilon u_r')\right]_{r=1} = \epsilon\left[r\frac{\partial}{\partial r}\left(\frac{\hat{u}_\theta'}{r}\right) + \frac{1}{r}\frac{\partial\hat{u}_r'}{\partial\theta}\right]_{r=1}, \tag{24d}$$

$$\hat{u}_r', \hat{u}_\theta'|_{r\to 0} < \infty. \tag{24e}$$

We now introduce the perturbation scheme $\boldsymbol{u}' = \boldsymbol{u}_1 + \epsilon\boldsymbol{u}_2 + \ldots$, $p' = p_1 + \epsilon p_2 + \ldots$, where u' and p' are dimensionless variables with the asterisks dropped. In view of (16) and (18) we may write

$$\boldsymbol{u} = A_{00}\boldsymbol{u}_0 + \epsilon\boldsymbol{u}_1 + \epsilon^2\boldsymbol{u}_2 + \ldots, \tag{25a}$$

$$p = A_{00}p_0 + \epsilon p_1 + \epsilon^2 p_2 + \ldots, \tag{25b}$$

where $\boldsymbol{u}$ and p also are dimensionless. It is not necessary to perturb $\boldsymbol{u}'$ because an exact solution of the liquid-side momentum equation can be obtained, as will be shown later.

By substituting (25) into (20–24) and equating powers in ϵ we obtain the following.

Order ϵ^0:

$$\nabla\cdot\boldsymbol{u}_0 = 0, \tag{26}$$

$$A_{00}\,\boldsymbol{u}_0\cdot\nabla\boldsymbol{u}_0+\nabla p = \nabla^2\boldsymbol{u}_0, \tag{27}$$

with boundary conditions

$$u_{0r}|_{r\to\infty} = u_{0\theta}|_{r\to\infty} = 0, \quad u_{0r}|_{r=1} = 1, \quad u_{0\theta}|_{r=1} = 0, \tag{28a, b, c}$$

The solution for the above set is

$$\boldsymbol{u}_0 = \frac{1}{r^2}\hat{\boldsymbol{r}}. \tag{29}$$

The liquid phase does not have any internal flow field to this order.

Order ϵ^1:

$$\nabla\cdot\boldsymbol{u}_1 = 0, \tag{30}$$

$$\nabla\cdot\hat{\boldsymbol{u}}' = 0, \tag{31}$$

$$A_{00}(\boldsymbol{u}_0\cdot\nabla\boldsymbol{u}_1+\boldsymbol{u}_1\cdot\nabla\boldsymbol{u}_0)+\nabla p_1 = \nabla^2\boldsymbol{u}_1, \tag{32}$$

$$Re\,\hat{\boldsymbol{u}}'\cdot\nabla\hat{\boldsymbol{u}}'+\nabla\hat{p}' = \nabla^2\hat{\boldsymbol{u}}', \tag{33}$$

with boundary conditions

$$\left.\begin{aligned} u_{1r}|_{r\to\infty} &= \cos\theta,\\ u_{1\theta}|_{r\to\infty} &= -\sin\theta, \end{aligned}\right\} \tag{34a}$$

$$\left.\begin{aligned} u_{1r}|_{r=1} &= A_{01}+A_{11}\cos\theta,\\ \hat{u}'_r|_{r=1} &= 0, \end{aligned}\right\} \tag{34b}$$

$$u_{1\theta}|_{r=1} = \hat{u}'_\theta|_{r=1}, \tag{34c}$$

$$\phi_\mu\left[r\frac{\partial}{\partial r}\left(\frac{u_{1\theta}}{r}\right)+\frac{1}{r}\frac{\partial u_{1r}}{\partial\theta}\right]_{r=1} = \left[r\frac{\partial}{\partial r}\left(\frac{\hat{u}'_\theta}{r}\right)+\frac{1}{r}\frac{\partial\hat{u}'_r}{\partial\theta}\right]_{r=1}, \tag{34d}$$

$$\hat{u}'_\theta, \hat{u}'_r|_{r\to 0} < \infty. \tag{34e}$$

We introduce stream functions ψ_1 and $\hat{\psi}$ for the gas and the liquid phases respectively. The continuity equations (30)–(31) are identically satisfied by letting the velocities be

$$\left.\begin{aligned} u_{1r} &= \frac{1}{r^2\sin\theta}\frac{\partial\psi_1}{\partial\theta},\\ u_{1\theta} &= -\frac{1}{r\sin\theta}\frac{\partial\psi_1}{\partial r} \end{aligned}\right\} \quad (1 < r < \infty), \tag{35}$$

$$\left.\begin{aligned} \hat{u}'_r &= \frac{1}{r^2\sin\theta}\frac{\partial\hat{\psi}}{\partial\theta},\\ \hat{u}'_\theta &= -\frac{1}{r\sin\theta}\frac{\partial\hat{\psi}}{\partial r} \end{aligned}\right\} \quad (0 \leqslant r < 1). \tag{36}$$

With these velocities, the momentum equations (32), (33) become

$$\mathrm{D}^4\psi_1 = A_{00}\frac{1}{r}\left(\frac{\partial}{\partial r}-\frac{2}{r}\right)\mathrm{D}^2\psi_1 \quad (1<r<\infty), \tag{37}$$

$$\mathrm{D}^4\hat{\psi} = \widehat{Re}\left\{\frac{1}{r^2}\frac{\partial(\hat{\psi},\mathrm{D}^2\hat{\psi})}{\partial(r,\bar{\mu})}+\frac{2}{r}(\mathrm{D}^2\hat{\psi})\left[\frac{\bar{\mu}}{(1-\bar{\mu}^2)}\frac{\partial\hat{\psi}}{\partial r}+\frac{1}{r}\frac{\partial\hat{\psi}}{\partial\bar{\mu}}\right]\right\} \quad (0\leqslant r<1), \tag{38}$$

where
$$\bar{\mu}=\cos\theta,\quad \mathrm{D}^2=\frac{\partial^2}{\partial r^2}+\frac{1-\bar{\mu}^2}{r^2}\frac{\partial^2}{\partial\bar{\mu}^2}.$$

The boundary conditions (34) become

$$\psi_1|_{r\to\infty}=\tfrac{1}{2}r^2(1-\bar{\mu}^2), \tag{39a}$$

$$\left.\begin{aligned} -\frac{1}{r^2}\frac{\partial\psi}{\partial\bar{\mu}}\bigg|_{r=1} &= A_{01}+A_{11}\bar{\mu},\\ -\frac{1}{r^2}\frac{\partial\hat{\psi}}{\partial\bar{\mu}}\bigg|_{r=1} &= 0,\end{aligned}\right\} \tag{39b}$$

$$\frac{\partial\psi_1}{\partial r}\bigg|_{r=1}=\frac{\partial\hat{\psi}}{\partial r}\bigg|_{r=1}, \tag{39c}$$

$$\phi_\mu\left[\frac{r}{\sin\theta}\frac{\partial}{\partial r}\left(\frac{1}{r^2}\frac{\partial\psi_1}{\partial r}\right)+\frac{1}{r^2}\frac{\partial}{\partial\theta}\left(\frac{1}{\sin\theta}\frac{\partial\psi_1}{\partial\theta}\right)\right]_{r=1}$$
$$=\left[\frac{r}{\sin\theta}\frac{\partial}{\partial r}\left(\frac{1}{r}\frac{\partial\hat{\psi}}{\partial r}\right)+\frac{1}{r^2}\frac{\partial}{\partial\theta}\left(\frac{1}{\sin\theta}\frac{\partial\hat{\psi}_1}{\partial\theta}\right)\right]_{r=1}, \tag{39d}$$

$$\frac{1}{r^2}\hat{\psi}|_{r\to 0}<\infty. \tag{39e}$$

In view of (39*a*–*c*) we assume solutions of the form

$$\psi_1=-A_{01}\bar{\mu}+\tfrac{1}{2}f(r)\,(1-\bar{\mu}^2), \tag{40}$$

$$\hat{\psi}=\tfrac{1}{2}g(r)\,(1-\bar{\mu}^2). \tag{41}$$

The substitution of (40) into (37) yields

$$\left[\frac{\mathrm{d}^2}{\mathrm{d}r^2}-\frac{A_{00}}{r}\left(\frac{\mathrm{d}}{\mathrm{d}r}-\frac{2}{r}\right)-\frac{2}{r^2}\right]\left[\frac{\mathrm{d}^2}{\mathrm{d}r^2}-\frac{2}{r^2}\right]f(r)=0. \tag{42}$$

The general solution of (42) is

$$f(r)=\frac{B}{r}+C\left[\frac{A_{00}}{r}\int_{1/A_{00}}^{r/A_{00}}(\xi^4+\xi^3)\,\mathrm{e}^{-1/\xi}\,\mathrm{d}\xi\right]+Er^4+Fr^2, \tag{43}$$

where B, C, E and F are integration constants. The substitution of (41) into (38) leads to

$$\left(\frac{\mathrm{d}^2}{\mathrm{d}r^2}-\frac{2}{r^2}\right)^2 g(r)=0, \tag{44a}$$

$$\left(\frac{\mathrm{d}}{\mathrm{d}r}-\frac{2}{r}\right)\left(\frac{\mathrm{d}^2}{\mathrm{d}r^2}-\frac{2}{r}\right)g(r)=0. \tag{44b}$$

A solution of (44) satisfying (39*c*, *e*) is

$$g(r) = \hat{B}(r^4 - r^2), \tag{45}$$

or

$$\hat{\psi} = \tfrac{1}{2}\hat{B}(r^4 - r^2)(1-\bar{\mu}^2). \tag{46}$$

which is Hill's spherical vortex with strength $\widehat{Re}\,\hat{B}$.

To determine the behaviour of the gas-phase solution at infinity, we need to carry out an asymptotic expansion of the integral in (43). With $x = r/A_{00}$, the integral may be written as

$$h(x) = \frac{1}{x}\int_{1/A_{00}}^{x} (\xi^4 + \xi^3)\,\mathrm{e}^{-1/\xi}\,\mathrm{d}\xi. \tag{47}$$

Successive integration by parts leads to the following behaviour for large x:

$$h(x) \sim \frac{1}{5x}[x^5 + x^4 - \tfrac{1}{3}x^3 + \tfrac{1}{6}x^2 - \tfrac{1}{8}x + O(\log x)]\,\mathrm{e}^{-1/x}. \tag{48}$$

The expansion of $\mathrm{e}^{-1/x}$ for large x gives

$$h(x) \sim \tfrac{1}{5}x^4 - \tfrac{1}{6}x^2 + \tfrac{1}{6}x - \tfrac{1}{8} + O\left(\frac{1}{x}\log x\right). \tag{49}$$

The behaviour of $h(x) = O(x^4)$ is not proper for a finite velocity field as $r = A_{00}\,x \to \infty$. However, x^4 and x^2 are two linearly independent solutions of (42) in addition to (47). We may therefore subtract $(\tfrac{1}{5}x^4 - \tfrac{1}{6}x^2)$ from $h(x)$ and still maintain linear independence.

Thus, in order for ψ_1 to behave like a uniform stream at infinity, $f(r)$ takes the form

$$f(r) = r^2 + \frac{B}{r} + C\left[\frac{A_{00}}{r}\int_{1/A_{00}}^{r/A_{00}} (\xi^4+\xi^3)\,\mathrm{e}^{-1/\xi}\,\mathrm{d}\xi - \frac{1}{5}\left(\frac{r}{A_{00}}\right)^4 + \frac{1}{6}\left(\frac{r}{A_{00}}\right)^2\right]. \tag{50}$$

After satisfying the remaining boundary conditions (39*b*–*d*) we obtain

$$B = \frac{(1-A_{11})[1-\tfrac{1}{5}(3+2\phi_\mu) - (1+A_{00}-\tfrac{1}{3}\phi_\mu A_{00}^2)\,\mathrm{e}^{-A_{00}}] + 2A_{11}(-\tfrac{1}{5}+\tfrac{1}{6}A_{00}^2)}{-1+\tfrac{1}{6}(3+2\phi_\mu)A_{00}^2 + (1+A_{00}-\tfrac{1}{3}\phi_\mu A_{00}^2)\,\mathrm{e}^{-A_{00}}}, \tag{51}$$

$$C = \frac{-[(3+2\phi_\mu) - A_{11}(1+2\phi_\mu)]A_{00}^4}{-1+\tfrac{1}{6}(3+2\phi_\mu)A_{00}^2 + (1+A_{00}-\tfrac{1}{3}\phi_\mu A_{00}^2)\,\mathrm{e}^{-A_{00}}}, \tag{52}$$

$$\hat{B} = \phi_\mu\left\{\frac{(1-A_{11})[1-\tfrac{1}{3}A_{00}^2 - (1+A_{00}+\tfrac{1}{6}A_{00}^2)\,\mathrm{e}^{-A_{00}}] + \tfrac{1}{3}A_{00}^2(1-\mathrm{e}^{-A_{00}})}{-1+\tfrac{1}{6}(3+2\phi_\mu)A_{00}^2 + (1+A_{00}-\tfrac{1}{3}\phi_\mu A_{00}^2)\,\mathrm{e}^{-A_{00}}}\right\}. \tag{53}$$

The complete dimensionless stream function for the gas phase is thus given by

$$\psi = -A_{00}\bar{\mu} + \epsilon[-A_{01}\bar{\mu} + \tfrac{1}{2}f(r)(1-\bar{\mu}^2)] + O(\epsilon^2). \tag{54}$$

For the liquid phase the stream function is given by (46).

The dimensionless velocities may now be written as

$$u_r = A_{00}\frac{1}{r^2} + \epsilon\left\{\frac{A_{01}}{r^2} + \left\{1 + \frac{B}{r^3} + \frac{C}{r^2}\left[\frac{A_{00}}{r}\int_{1/A_{00}}^{r/A_{00}}(\xi^4+\xi^3)\,\mathrm{e}^{-1/\xi}\,\mathrm{d}\xi - \frac{1}{5}\left(\frac{r}{A_{00}}\right)^4 + \frac{1}{6}\left(\frac{r}{A_{00}}\right)^2\right]\right\}\cos\theta\right\}, \tag{55a}$$

$$u_\theta = -\tfrac{1}{2}\epsilon\left\{2-\frac{B}{r^3}+\frac{C}{r^2}\left\{-\frac{A_{00}}{r}\int_{1/A_{00}}^{r/A_{00}}(\xi^4+\xi^3)\,e^{-1/\xi}\,d\xi\right.\right.$$

$$\left.\left.+\left[\left(\frac{r}{A_{00}}\right)^4+\left(\frac{r}{A_{00}}\right)^3\right]e^{-A_{00}/r}-\frac{4}{5}\left(\frac{r}{A_{00}}\right)^4+\frac{1}{3}\left(\frac{r}{A_{00}}\right)^2\right\}\right\}\sin\theta, \quad (55b)$$

$$\hat{u}_r = \widehat{Re}\,\hat{B}(r^2-1)\cos\theta, \quad (55c)$$

$$\hat{u}_\theta = -\widehat{Re}\,\hat{B}(2r^2-1)\cos\theta. \quad (55d)$$

4. Drag-force calculation

The drag force on the liquid drop consists of contributions from the viscous stresses, the pressure and the momentum flux at the interface. The viscous drag in dimensionless form is

$$F_\mu^* = \frac{F_\mu}{\mu U_\infty R} = \frac{2\pi}{\epsilon}\int_0^\pi [\sigma_{rr}\cos\theta - \sigma_{r\theta}\sin\theta]_{r=1}\sin\theta\,d\theta, \quad (56)$$

where σ_{rr} and $\sigma_{r\theta}$ are the viscous stresses. In terms of the dimensionless velocities,

$$F_\mu^* = \frac{2\pi}{\epsilon}\int_0^\pi\left\{2\frac{\partial u_r}{\partial r}\cos\theta-\left[r\frac{\partial}{\partial r}\left(\frac{u_\theta}{r}\right)+\frac{1}{r}\frac{\partial u_r}{\partial\theta}\right]\sin\theta\right\}_{r=1}\sin\theta\,d\theta$$

$$= \frac{4\pi C}{3}\left[\left(\frac{2}{A_{00}^4}+\frac{2}{A_{00}^3}+\frac{1}{A_{00}^2}\right)e^{-A_{00}}-\frac{2}{A_{00}^4}\right]$$

$$= -\frac{4\pi}{3}\left\{\frac{[(3+2\phi_\mu)-A_{11}(1+2\phi_\mu)]\,[(2+2A_{00}+A_{00}^2)\,e^{-A_{00}}-2]}{-1+\frac{1}{6}(3+2\phi_\mu)A_{00}^2+(1+A_{00}-\frac{1}{3}\phi_\mu A_{00}^2)\,e^{-A_{00}}}\right\}. \quad (57)$$

To calculate the pressure drag F_p we first obtain the pressure distribution using the momentum equation. The leading-order term p_0 makes no contribution to the drag. Only p_1, which is obtained by integrating the θ-component of (32), is used. In dimensionless form the θ-momentum equation is

$$\frac{\partial p_1}{\partial\theta} = \left(\nabla^2 u_{1\theta}+\frac{2}{r}\frac{\partial u_{1r}}{\partial\theta}-\frac{u_{1\theta}}{r}\right)-A_{00}\left(\frac{\partial u_{1\theta}}{\partial r}+\frac{u_{1\theta}}{r}\right). \quad (58)$$

Integration with respect to θ gives

$$p_1|_{r=1} = \epsilon\cos\theta\left\{-(1+B)A_{00}+C\left[\left(\frac{2}{A_{00}^4}+\frac{1}{A_{00}^3}\right)e^{-A_{00}}-\frac{2}{A_{00}^4}+\frac{6}{5A_{00}^3}-\frac{1}{6A_{00}}\right]\right\}+G, \quad (59)$$

where G is a constant. The dimensionless pressure drag is

$$F_p^* = \frac{2\pi}{\epsilon}\int_0^\pi(-p_1|_{r=1}\cos\theta)\sin\theta\,d\theta$$

$$= \frac{4\pi}{3}\left\{A_{00}A_{11}-C\left[\left(\frac{2}{A_{00}^4}+\frac{1}{A_{00}^3}\right)e^{-A_{00}}-\frac{2}{A_{00}^4}+\frac{1}{A_{00}^3}\right]\right\}$$

$$= \frac{4\pi}{3}\left\{A_{00}A_{11}+\frac{[(3+2\phi_\mu)-A_{11}(1+2\phi_\mu)]\,[(2+A_{00})\,e^{-A_{00}}+A_{00}-2]}{-1+\frac{1}{6}(3+2\phi_\mu)A_{00}^2+(1+A_{00}-\frac{1}{3}\phi_\mu A_{00}^2)\,e^{-A_{00}}}\right\}. \quad (60)$$

The force $F_m^* = F_m/\mu U_\infty R$ due to the momentum flux at the interface is given by

$$F_m^* = \frac{2\pi}{\epsilon}\int_0^\pi -[u_r u_r \cos\theta - u_r u_\theta \sin\theta]_{r=1} \sin\theta \, d\theta. \tag{61}$$

We include the terms only up to the first order to obtain

$$F_m^* = -\frac{4\pi}{3}\left\{3A_{00} + A_{00}A_{01} + C\left[\left(\frac{1}{A_{00}^3} + \frac{1}{A_{00}^2}\right)e^{-A_{00}} - \frac{1}{A_{00}^3} + \frac{1}{2A_{00}}\right]\right\}, \tag{62}$$

which is equal to

$$F_m^* = \frac{4\pi}{3}\left\{-A_{00}(3+A_{11}) + \frac{[(3+2\phi_\mu) - A_{11}(1+2\phi_\mu)]\,[(A_{00}+A_{00}^2)\,e^{-A_{00}} - A_{00} + \frac{1}{2}A_{00}^3]}{-1+\frac{1}{6}(3+2\phi_\mu)A_{00}^2 + (1+A_{00}-\frac{1}{3}\phi_\mu A_{00}^2)\,e^{-A_{00}}}\right\} \tag{63}$$

The total drag is the sum $F^* = F^* + F_p^* + F_m^*$ given by

$$\begin{aligned} F^* &= -\frac{4\pi}{3}\left\{3A_{00} + \frac{C}{2A_{00}}\right\} \\ &= \frac{4\pi}{3}\left\{-3A_{00} + \frac{\frac{1}{2}[(3+2\phi_\mu) - A_{11}(1+2\phi_\mu)]\,A_{00}^3}{-1+\frac{1}{6}(3+2\phi_\mu)A_{00}^2 + (1+A_{00}-\frac{1}{3}\phi_\mu A_{00}^2)\,e^{-A_{00}}}\right\}. \end{aligned} \tag{64}$$

A calculation of the total drag at infinity yields an identical expression.

5. Identification of a new singularity

In view of the usefulness of singularity distributions in the description of many types of flows (see e.g. Johnson & Wu 1979; Wu & Yates 1976), we have paid special attention to the identification of a new singularity. For this purpose it is convenient to associate a source strength $m = 4\pi A_0 R^2$ with the uniform radial field. In addition, A_{01} and A_{11} are set equal to zero. The dimensional stream function $\Psi = \psi R^2$ may now be written as

$$\Psi = -m\cos\theta + \tfrac{1}{2}\epsilon\left\{r^2 + \frac{BR^3}{r} + CR^2\left[\frac{1}{\zeta}\int_{\zeta_0}^{\zeta}(\xi^4+\xi^3)\,e^{-1/\xi}\,d\xi - \tfrac{1}{5}\zeta^4 + \tfrac{1}{6}\zeta^2\right]\right\}\sin^2\theta, \tag{65}$$

where r is the dimensional radial coordinate, $\zeta = 4\pi r\nu/m$ and $\zeta_0 = 4\pi R\nu/m$. Here the first term represents a point source; the second, a uniform stream, and the third, a doublet. The last term is proportional to

$$S = \frac{3m}{16\pi^2\nu\mu}\left[\frac{1}{\zeta}\int_{\zeta_0}^{\zeta}(\xi^4+\xi^3)\,e^{-1/\xi}\,d\xi - \tfrac{1}{5}\zeta^4 + \tfrac{1}{6}\zeta^2\right]\sin^2\theta. \tag{66}$$

This result represents a new singularity in which both the inertial and the viscous forces are accounted for. At large distances from the origin ($r \to \infty$) this singularity behaves like

$$S \sim \frac{1}{8\pi\mu} r\sin^2\theta, \tag{67}$$

which is a Stokeslet. The singularity S in (66) behaves also like a Stokeslet in the special case of A_0 becoming vanishingly small. This type of behaviour is to be expected because for A_0 becoming small the entire flow field collapses to the Stokes-flow limit.

In (66) ζ_0 may be arbitrarily chosen. It is quite clear that changing ζ_0 is equivalent to adding (or subtracting) a doublet to the singularity. The result is valid for both a source and a sink. In the case of a sink, ζ_0 must be non-zero for the integral to exist.

The flow field for the translation of a liquid drop or a rigid sphere with a strong radial field may be constructed by superimposing a point source and a doublet on the singularity S. The new singularity is particularly important in that it may be used to construct several other types of flows for which the viscous as well as the inertial effects may be significant.

6. Results and discussion

In this section we examine the interesting features resulting from the analysis. The flow streamlines are plotted for typical cases and their behaviour is discussed. The various factors governing the drag force and the strength of the internal vortex are ascertained.

6.1. *The flow field*

For illustrative purposes the streamlines of the flow corresponding to $A_{00} = \pm 2$, $A_{01} = \mp 0.25$, $\phi_\mu = 0.1$ and $\epsilon = 0.5$ are plotted in figure 2. For radially outward normal velocity ($A_{00} > 0$), streamlines emanate from the surface and follow the uniform stream. Near the front of the drop, the radial flow and the uniform stream oppose each other. As a result a stagnation point is formed there as shown in figure 2. For the inward flow ($A_{00} < 0$) a stagnation point is similarly formed near the rear of the drop. In this case, some of the streamlines from the uniform stream end on the surface of the drop.

For both $A_{00} > 0$ and $A_{00} < 0$ the flow field inside the drop is Hill's spherical vortex. Only the strength of the vortex is different. This will be discussed in §6.3.

6.2. *The drag force*

The expression for the drag force given by (64) is plotted in figure 3. We notice that for an outward radial velocity, with its maximum at the front, there is a decrease in the drag with increasing A_{00} until a minimum is reached. Subsequently the drag increases with an asymptotic behaviour like

$$F^* \sim -4\pi \frac{1+2\phi_\mu}{3+2\phi_\mu} A_{00} \left\{ A_{11} + \left[\frac{A_{11}}{(3+2\phi_\mu)} + \frac{1}{(1+2\phi_\mu)} \right] \frac{6}{A_{00}^2} + \ldots \right\}, \tag{68}$$

where $A_{11} < 0$. The decrease in drag is due to the vorticity being convected away from the surface, and due to the reduction in the pressure drop from the front to the rear stagnation points. In fact, for a sufficiently large radial velocity, we have a larger pressure at the rear than at the front, giving rise to a negative pressure drag. This may be explained by an examination of the negative contribution of the inertial term $-\frac{1}{2}\rho \boldsymbol{u} \cdot \boldsymbol{u}$ towards the pressure distribution. With the maximum radial velocity at the front of the drop, a strong inertial effect would lead to a higher pressure at the rear. A competing mechanism opposing the motion is the normal reaction of the momentum flux leaving the surface. With the maximum flux at the front of the drop, the recoil increases the drag. With increasing A_{00} this force becomes the dominating effect, resulting in an increasing total drag. In the special case of a uniform radially outward velocity ($A_{11} = 0$), the drag continues to decrease with increasing A_{00}. We further notice that with sufficient non-uniformity in the radial velocity ($A_{11} \gtrsim 3$) the drag force increases with decreasing drop viscosity. Such an effect is apparent from the examination of (64). This feature is also exhibited in the case of Stokes flow.

Next, for an inward normal velocity ($A_{00} < 0$), the drag on the drop increases monotonically with increasing $-A_{00}$. Here the vorticity is convected towards the

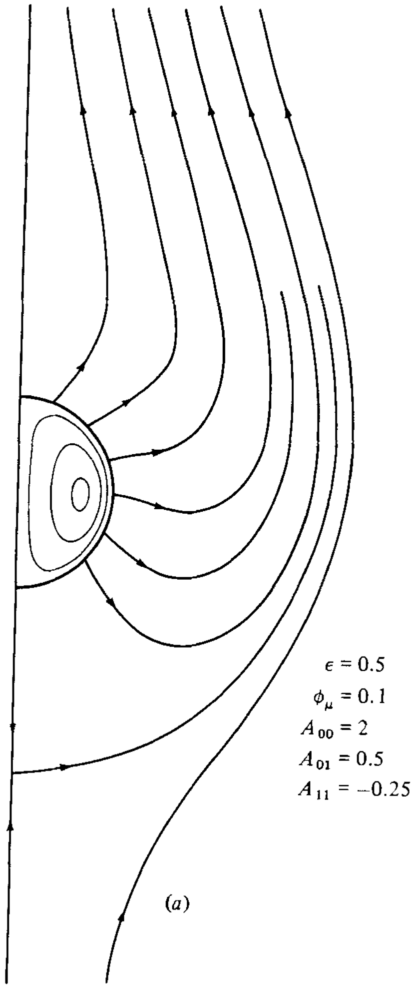

Figure 2 (a). For caption see facing page.

surface, and hence the viscous drag increases. The surface pressure variation causes a reduction in the drag force as it does in the case of the outward velocity. However, the momentum deposited non-uniformly on the surface creates a stronger net force opposing motion. It is interesting to note that, for both outward and inward normal velocities, the net momentum flow at the surface opposes the motion when the maximum magnitude of the velocity is at the front. In the former case the force is due to the recoil of the momentum leaving, while in the latter case it is due to the impact of the inward flux. This result is mathematically evident from the positive value of $u_r u_r$ in (61).

The interfacial momentum transport also affects the drag through the tangential momentum convected radially inwards or outwards. This is obvious from the non-zero $u_r u_\theta$ term in (61). For a solid sphere this effect is absent.

For the case in which the maximum of the radially outward velocity occurs at the rear stagnation point (e.g. the burning of the wake), a qualitative description of the flow is still possible from our analysis. By letting both A_{00} and A_{11} be positive we predict that the drag is reduced in conformity with experimental observation (see Baker 1970).

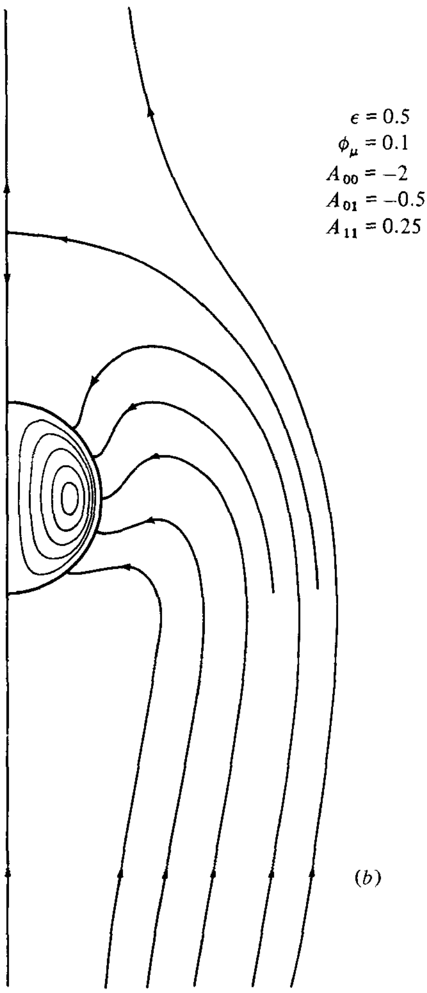

FIGURE 2. Flow streamlines for a moving drop with (*a*) outward and (*b*) inward radial velocities.

In the limit of letting A_{00} become vanishingly small in (64) we recover the results appropriate to Stokes flow. An asymptotic expansion for small A_{00} gives

$$F^* \sim 4\pi\left\{\frac{(3+2\phi_\mu)-A_{11}(1+2\phi_\mu)}{(2+2\phi_\mu)} + A_{00}\left\{\frac{(3+4\phi_\mu)}{16}\left[\frac{(3+2\phi_\mu)-A_{11}(1+2\phi_\mu)}{(1+\phi_\mu)^2}-1\right]\right\}+O(A_{00}^2)\right\}. \quad (69)$$

The first term in this expression is the total drag force for Stokes flow. The next term represents a departure from this approximation. It is clear from the first term that with Stokes flow the effect of the normal velocity only manifests itself through the angular dependence ($A_{11} \neq 0$). Gal-Or & Yaron (1973) applied a correction to the first term for small A_{00} by using Stokes-flow velocities to calculate the momentum flux at the interface. Their analysis did not yield our second term above because their

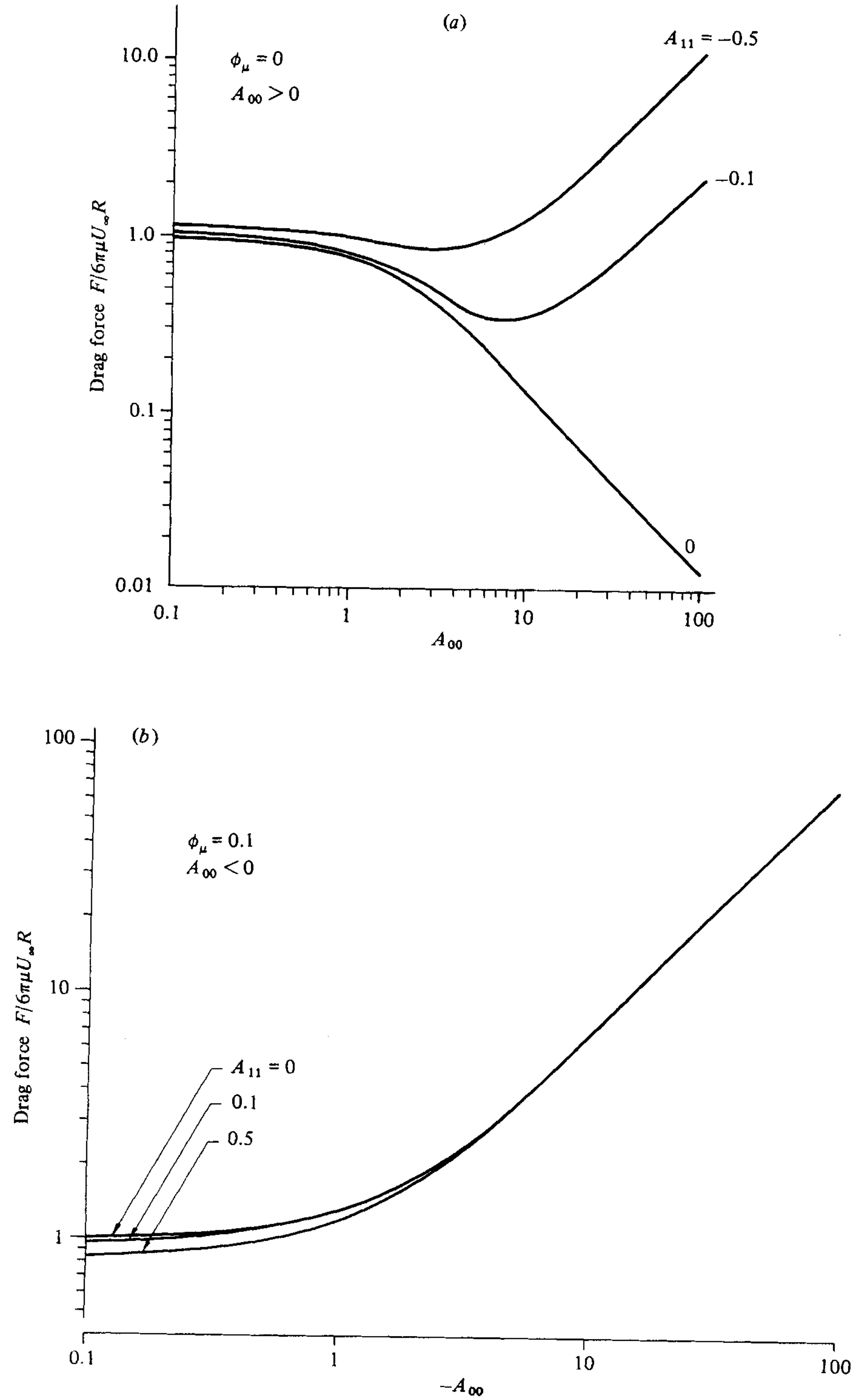

FIGURE 3. The drag force as a function of increasing radial velocity: (a) outward flow; (b) inward flow.

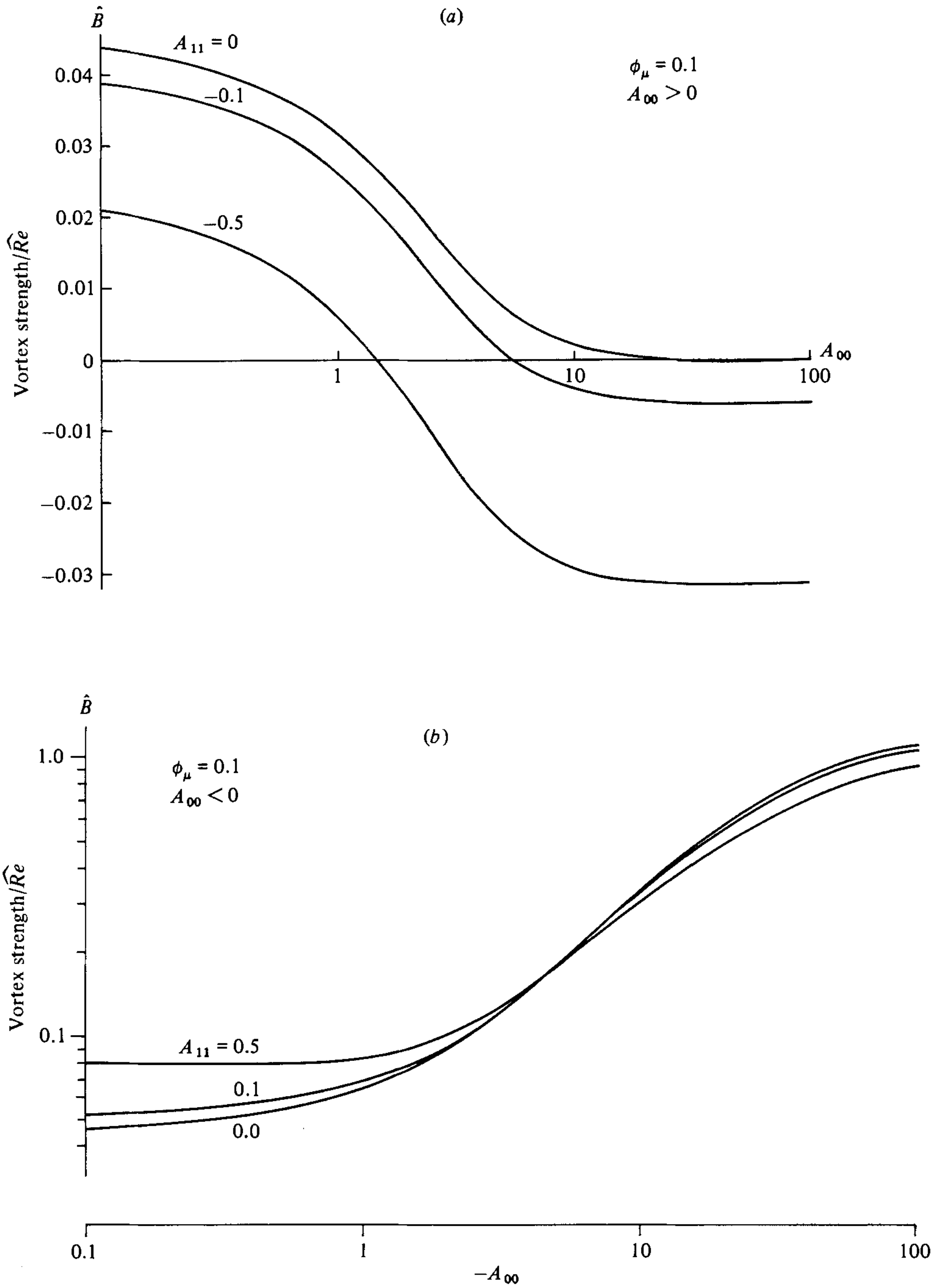

FIGURE 4. Variation of the strength of internal vortex with radial velocity: (*a*) outward flow; (*b*) inward flow.

correction $-\rho u_i u_j$, while accounting for the inertial effects, is apparently inconsistent with their Stokes-flow assumption, which neglects inertia in the velocity and pressure calculation.

6.3. *The internal circulation*

The internal circulation provides an important mechanism for the heat and/or mass transfer associated with moving drops. The strength of the internal vortex is therefore not only a highly useful parameter in the modelling of such systems, but is also necessary in the actual evaluation of the extent of transport. We find that for increasing radially outward velocity the strength of the vortex decreases. This is to be expected because of the reduced vorticity at the surface, as discussed earlier. For an inward normal velocity the strength increases. An expression for this strength is given by (53), and the numerical values are plotted in figure 4. A remarkable feature of the evaporating drop is that with a sufficiently large radial velocity the internal circulation vanishes. A further increase in A_{00} reverses the circulation. This very interesting result is due to the non-uniformity of the radial field, which, with its maximum at the front of the drop, provides a shear stress to oppose the usual circulation. With increasing radial velocity, the vorticity resulting from translation is convected away, while the shear stress due to the non-uniformity in the normal velocity persists. Consequently the internal circulation weakens to a point where the latter force dominates and causes a reversal. Further investigation into the time-dependent transition of the flow reversal is currently under way.

In the limit of A_{00} becoming vanishingly small we recover the vortex strength for Stokes flow. In the case of uniform normal velocity ($A_{11} = 0$), the result from Stokes flow shows no dependence on A_{00}. This is evident because the Stokes approximation does not include the inertial effects which are primarily responsible for altering the vortex strength.

The authors are very grateful to Dr Andrea Prosperetti (Istituto di Fisica, Milano, Italy) for valuable discussion on this paper, and to the referees who made useful suggestions. This research was partially supported by the National Science Foundation (MEA-8023861).

REFERENCES

BAKER, D. R. 1970 Analogical determination of drag coefficient of a burning drop in a freefall. Engineer's thesis, Department of Mechanical Engineering, University of Southern California.

CHUNG, J. N., AYYASWAMY, P. S. & SADHAL, S. S. 1983*a* Laminar condensation on a moving drop. Part 1. Singular perturbation technique. Unpublished manuscript.

CHUNG, J. N., AYYASWAMY, P. S. & SADHAL, S. S. 1983*b* Laminar condensation on a moving drop. Part 2. Numerical solutions. Unpublished manuscript.

CLIFT, R., GRACE, J. R. & WEBER, M. E. 1978 *Bubbles, Drops and Particles*. Academic.

FENDELL, F. E., SPRANKLE, M. L. & DODSON, D. S. 1966 Thin flame theory for a fuel drop in slow viscous flow. *J. Fluid Mech.* **26**, 267–280.

GAL-OR, B. & YARON, I. 1973 Diffusion drag upon slowly evaporating drops. *Phys. Fluids* **16**, 1826–1829.

HADAMARD, J. 1911 Mouvement permanent lent d'une sphère liquide et visqueuse dans un liquide visqueux. *C.R. Acad. Sci. Paris* **152**, 1735–1738.

HARPER, J. F. 1972 The motion of drops and bubbles through liquids. *Adv. Appl. Mech.* **12**, 59–129.

JOHNSON, R. E. & WU, T. Y. 1979 Hydrodynamics of low-Reynolds-number flow. Part 5. Motion of a slender torus. *J. Fluid Mech.* **95**, 263–277.

LAW, C. K. 1982 Recent advances in droplet evaporation and combustion. *Prog. Energy Combust. Sci.* **8**, 171–201.

RYBCZYNSKI, W. 1911 On the translatory motion of a fluid sphere in a viscous medium (in German). *Bull. Int. Acad. Pol. Sci. Lett. Cl. Sci. Math. Nat.* **A**, 40–46.

SCHNEIDER, W. 1981 Drag on droplets moving through their own vapour. Part I – Continuum flow. *PhysicoChem. Hydrodyn.* **2**, 135–141.

SAITO, S. 1913 *Sci. Rep. Tohoku Imp. Univ., Sendai, Japan* **2**, 179.

TAYLOR, T. D. & ACRIVOS, A. 1964 On the deformation and drag of a falling viscous drop at low Reynolds number. *J. Fluid Mech.* **18**, 466–476.

WU, T. Y. & YATES, G. 1977 Finite amplitude unsteady slender body flow theory. In *Unsteady Hydrodynamics of Marine Vehicles* (ed. R. E. E. Bishop, A. G. Parkinson & W. G. Price), pp. 517–528.